文章编号: 1001 - 9014(2017)04 - 0397 - 06

DOI:10.11972/j.issn.1001 - 9014.2017.04.004

Volatilization characteristics analysis of ammonia from soil by straw returning to the field based on the infrared spectroscopy technology

HE Ying[1,2,3*], ZHANG Yu-Jun[1,3], YOU Kun[1,3], GAO Yan-Wei[1,3], ZHAO Nan-Jing[1,3], LIU Wen-Qing[1,3]

(1. Key Laboratory of Environmental Optics& Technology, Anhui Institute of Optics and Fine Mechanics, the Chinese Academy of Sciences, Hefei 230031, China;
2. University of Science and Technology of China, Hefei 230026, China;
3. Key Laboratory of Optical Monitoring Technology for Environment, Hefei 230031, China)

Abstract: The infrared absorption spectral characteristics of ammonia were studied. Moreover, the quantitative inversion algorithm model was established, especially the correlation analysis and temperature correction function were optimized. The ammonia volatilization experiment was carried out in the demonstration area in Guoyang, Anhui in 2015 by the ammonia regional monitoring system based on Open-path Tunable Diode Laser Absorption Spectroscopy (OP-TDLAS). Then, ammonia dynamic volatilization character of corn and wheat straw returning to the field was studied. The monitoring results show that the ammonia concentration has a certain diurnal variation trend: it increased during the daytime and got to the maximum value at midday, then reduced gradually at night to the minimum. The typical hourly concentration varied from 0.6×10^{-3} to 1.34×10^{-3} mmol/mol in summer, and it varied from 1.14×10^{-3} to 1.82×10^{-3} mmol/mol in autumn. In autumn, the maximum daily average of ammonia volatilization from corn straw returning was 4.6×10^{-4} mmol/mol, and it was 1.7×10^{-3} mmol/mol from wheat straw returning in summer. The results indicate that the emission concentration rises significantly after more than one month of straw returning which has some certain seasonal difference in farmland scale. This infrared spectroscopy technology provides technical support for clarifying the ammonia emission rules in soil environment.

Key words: infrared laser absorption spectroscopy, ammonia volatilization, straw returning to the field, open-path monitoring, quantitative inversion algorithm

PACS: 42.62.Fi, 42.68.Ca, 88.05.Qr

基于红外光谱技术的秸秆还田环境下土壤氨挥发特征分析

何 莹[1,2,3*], 张玉钧[1,3], 尤 坤[1,3], 高彦伟[1,3], 赵南京[1,3], 刘文清[1,3]

(1. 中国科学院环境光学与技术重点实验室,安徽光学精密机械研究所,安徽 合肥 230031;
2. 中国科学技术大学,安徽 合肥 230026;
3. 安徽省环境光学监测技术重点实验室,安徽 合肥 230031)

摘要:研究氨近红外光谱特性并建立浓度反演算法模型,重点优化相关性分析和温度修正功能.利用开放式激光吸收光谱技术建立氨区域监测系统,于2015年在安徽涡阳秸秆还田示范区开展监测实验,研究玉米和小麦种植情况下的土壤氨挥发特征.研究结果表明,氨浓度具有日变化趋势:白天浓度上升在正午达到最高值,逐步降低到夜间至最小值.夏、秋季典型小时浓度变化范围为0.6×10^{-3} ~ 1.34×10^{-3} mmol/mol和1.14×10^{-3} ~ 1.82×10^{-3} mmol/mol,秋季玉米和夏季小麦秸秆还田的最大氨日均浓度为4.6×10^{-4} mmol/mol和1.7×10^{-3} mmol/mol,还田一个多月后氨浓度明显上升,并存在一定季节性差异.近红外光谱技术为明晰土壤氨排放规律提供了技术支持.

关 键 词:近红外激光吸收光谱;氨挥发;秸秆还田;开放式监测;浓度反演算法

中图分类号:O433.1 **文献标识码**:A

Received date: 2016-09-29, **revised date**: 2017-04-19 **收稿日期**:2016-09-29, **修回日期**:2017-04-19

Foundation items: Supported by the National Key Scientific Instrument and Equipment Development Projects (2012YQ22011902), the Special Foundation for Young Scientists of Hefei Institutes of Physical Science, Chinese Academy of Sciences (YZJJ201502)

Biography: HE Ying (1983-), female, Hefei China, assistant professor, master. Research area is gases monitoring in atmosphere with laser absorption spectroscopy.

* **Corresponding author**: E-mail: heying@aiofm.ac.cn

Introduction

In recent years, the method of straw returning to the field has been gradually adopted in China. Straw is one kind of effective farmland fertilizer for soil fertility improvement. Nevertheless straw returning to the field would affect soil respiration, bacteria activity and the physical-chemical characteristics of soil, which could influence the nitrogen exchange features between the earth and atmosphere. Ammonia (NH_3) is the most abundant alkaline trace gas in the atmosphere in addition to N_2O, which influences the quality of the regional air and atmospheric visibility. In addition, ammonia leads to ecosystem eutrophication and other environmental problems[1-5]. Thus, precise measurement of ammonia emission concentration with straw returning to the field to evaluate its environmental impact becomes an urgent problem in agricultural and environmental protection fields.

In China, the ammonia measurement methods used in farmland are local or indirect methods, such as chamber method, micrometeorology method, etc. Chamber method is used mainly for macroscopic description and observation of local soil. Micrometeorology method[6] is applied widely, but the observation requirement to underlying surface and atmospheric stability are harsh. Since ammonia emissions in farmland was influenced by comprehensive management mode (such as fertilization, irrigation, farming, straw returned style and environmental condition), it is necessary to establish a real-time monitoring method in farmland scale in order to acquire accurate ammonia volatilization information of soil.

These years, many optical methods have been applied to ammonia continuous measurement, such as chemical ionization mass spectrometry technique, photo-fragmentation laser-induced fluorescence technique, and Open-path Tunable Diode Laser Absorption Spectroscopy (OP-TDLAS) technology[7-8]. OP-TDLAS is one kind of non-contact rapid measurement technology with high sensitivity, high resolution and large scale measurement. Now-adays, many studies have demonstrated the accuracy of OP-TDLAS technology and its applicability for ammonia emission monitoring[9-10]. Moreover, some domestic institutions have carried out OP-TDLAS research[11-13], but there are only a few reports of ammonia emission measurements with straw returning by this technology in recent literatures.

In this paper, the infrared spectroscopy detection methods of ammonia concentration, especially the quantitative inversion algorithm, were studied, and the continuous monitoring experiment of ammonia volatilization by the OP-TDLAS monitoring system was carried out to obtain the precise characteristics of ammonia in the demonstration area in Guoyang, Anhui. Furthermore, the ammonia volatilization rules were analyzed on the typical condition of straw returning to the field with the effective working parameters.

1 Spectrum measurement principle and method

1.1 Measurement principle

Ammonia molecule has four vibrational modes: two parallel modes ν_1 and ν_2 which are symmetric, and two perpendicular modes ν_3 and ν_4 which are asymmetric and degenerate. In addition to the inversion-splittings, the ammonia spectroscopy is complicated by strong Coriolis effects between ν_2 and ν_4, and it has the main absorption bands at 1.5 μm. In the NIR, the perpendicular bands predominate in intensity. The total internal partition function $Q(T)$ is the sum of the valid state of all the energy level at temperature T, namely the number of average state in gas molecular system at this temperature. $Q(T)$ can be described classically as a product of the nuclear partition functions (Q_{nuc}), rotational partition functions (Q_{rot}), and vibrational partition functions (Q_{vib}), if the interactions between vibrations and rotations are neglected. In general, $Q(T)$ can be expressed approximately by a third-order polynomial, and the partition function values can be predicted by Hitran and Gamache database[14]. $Q(T)$ in Hitran underestimates the classical partition function as ignoring the Q_{vib} contribution.

$$Q(T) = a + bT + cT^2 + dT^3. \quad (1)$$

Table 1 The partition function values predicted by Hitran and Gamache

表 1 Hitran and Gamache 数据库预测的配分函数

	Hitran		Gamache	
Coefficient	$70 < T < 500$ K	$500 < T < 1500$ K	$70 < T < 500$ K	$500 < T < 1\,500$ K
a	-42.037	-471.39	-62.293	-0.59594e4
b	2.597 6	5.403 5	3.091 5	32.387
c	0.013 073	6.4491e-3	9.4575e-3	-4.0459e-2
d	-6.2223e-6	-7.2674e-7	1.8416e-6	3.1843e-5

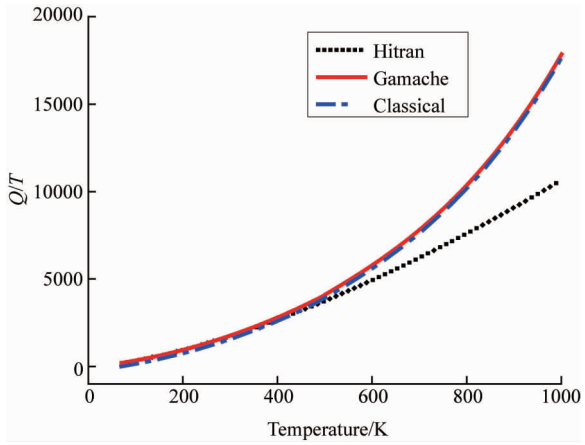

Fig. 1 Partition function curve

图 1 配分函数曲线

As absorption line strength $S(T)$ is related to the temperature T, it can be expressed by $S(T_0)$ at the standard temperature T_0:

$$S(T) = S(T_0)\frac{Q(T_0)}{Q(T)}\left(\frac{T_0}{T}\right)\exp\left[-\frac{hcE''}{k}\left(\frac{1}{T}-\frac{1}{T_0}\right)\right]\times \left[1-\exp\left(\frac{-hc\upsilon_0}{kT}\right)\right]\Big/\left[1-\exp\left(\frac{-hc\upsilon_0}{kT_0}\right)\right] \quad (2)$$

where E'' is the energy at molecular low level, h is the

Planck's constant (6.626×10^{-27} erg · s), k is the Boltzmann's constant (1.38×10^{-16} erg/K), c is the speed of light in vacuum. As OP-TDLAS obeys the Beer-Lambert law, the laser with original laser intensity I_0 and frequency ν goes through the absorbing medium, and concentration c can be expressed as:

$$c = \frac{A}{S(T)PL} \quad , \quad (3)$$

where P is the partial pressure, L is the optical path length, A is the integrated absorbance[15]. Replacing A with a reasonable minimum detectable absorbance (MDA), the minimum detectivity $X_{j,\min}$ of specie j can be expressed as:

$$X_{j,\min} = \frac{\mathrm{MDA}}{S(T)PL} \quad . \quad (4)$$

1.2 Concentration inversion algorithm

The effective spectral resolution and feature extraction is the focus for accurate concentration inversion. First of all, the incident intensity baseline was got by nonlinear polynomial fitting, the absorption part and no absorption part should be chosen seriously based on spectral feature extraction. Then, the absorbance curve was extracted and optical intensity normalization was carried out. Thirdly, the correlation between the extracted absorbance in measurement and the reference spectral absorbance was analyzed, so the invalid data of low correlation coefficient was removed. Moreover, the non-linear fitting of Lorentzian lineshape function was used to remove distort absorbance caused by atmospheric turbulence effect in open-path monitoring. At last, the absorption peak and integral area were obtained to calculate integrated absorbance A and gas concentration with line strength $S(T)$ correction. Comparing with the previous study of concentration inversion algorithm, the correlation analysis and temperature correction function were optimized. The flow diagram of concentration inversion algorithm is shown in Fig. 2.

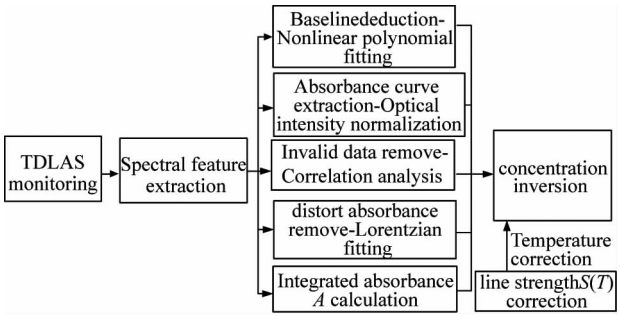

Fig. 2　Flow chart of concentration inversion algorithm
图 2　浓度反演算法流程图

As the optical path length is long in open-path monitoring, the detection signal is often affected by atmospheric turbulence. The correlation coefficient (R^2) between the measured absorbance spectral signal ($y[n]$) and the reference spectral signal ($x[n]$) in the main absorption region can be calculated as Eq. 5:

$$R(x,y) = \frac{\sum_{n=1}^{N} x[n] * y[n]}{\sqrt{\sum_{n=1}^{N} x^2[n] * \sum_{n=1}^{N} y^2[n]}} \quad . \quad (5)$$

We used different absorbance signals to test this algorithm function and calculate the measurement error, as shown in Fig. 3. It is concluded that the higher the correlation coefficient is, the lower the measurement error becomes. When the correlation coefficient is greater than 85%, the relative error is less than 5% to satisfy signal detection requirement. So, the effective measured absorbance signal for accuracy concentration inversion was selected, and other invalid signal was directly filtered by the system software.

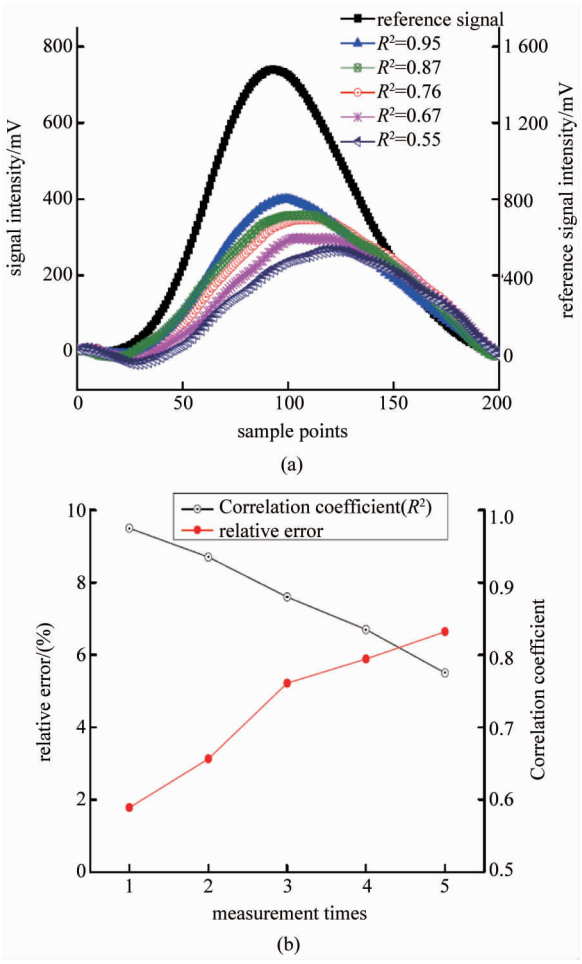

Fig. 3　(a) The measured absorbance spectra of different correlation coefficient, (b) the measurement relative error of different correlation coefficient
图 3　(a) 不同相关系数下的测量吸收光谱信号, (b) 不同相关系数下的测量相对误差

During the research, the absorption line strength $S(T)$ is calculated as 0.01932 at 288 K and 0.016 04 at 308 K respectively (if we use the $S(T)$ at 288K for concentration inversion at 308 K, the calculation error is high), so the concentration inversion with temperature correction is important to reduce the calculation error.

2 Measurement system

The OP-TDLAS ammonia monitoring system was set-up in our lab which mainly comprises of a tunable infrared diode laser at 1.53 μm and its controller, the electronic elements, and optical elements(telescope & retro-reflector), the details were summarized in literatures[16] of our group. The multiple reflection cell whose optical path length is 35.8 m was connected to this OP-TDLAS system to build the detection path. Then, we inflated a set of distributed ammonia gases into the cell controlled at 308 K. The absorbance spectral signal by profile fitting was obtained and the inversion cycle was about 1s to achieve fast detection. Then the inversion results were compared to analyze the system accuracy by relative error, as shown in Fig. 4 and Table 2. The results show that the maximum of relative error before and after temperature correction is 5.78% and 2.75%, respectively, so the inversion concentration algorithm with temperature correction is more accurate.

The detection sensitivity of OP-TDLAS system depends on the optical path length and the gas species. According to the Beer-Lambert law, the detection limit is inversely proportional to the path length. This system minimum detectivity is about 4.0×10^{-3} mmol/mol · m by the stability experiment and standard deviation calculation when SNR = 1.

3 Experiment environment

3.1 Measurement parameters

For the OP-TDLAS system, the poor detection limit for short path length is inadequate to meet the monitoring requirement of trace NH_3. However, the alignment of the optical path is not always stable for effectively monitoring in large scale because that the turbulent fluctuations caused by wind is quite complex. As a matter of experience, the optical path length was chosen about 400 m for NH_3 detection with OP-TDLAS. According to this, the corresponding system detection limit is about 1.0×10^{-5} mmol/mol.

The path height is defined as the average of the path center height of the transmitter telescope and reflector. Generally, there are heights at which the influence of atmospheric stability on concentration is minimized, which can be regarded as the best measurement position. It is suggested that concentration measurements should be made at a suitable height, about 2 ~ 2.5 m, for a homogenous surface layer to avoid detection at the plume edge. In addition, the measurement is not affected by the plant canopy, the obstructions and other factors. Thus, the optical path height was chosen about 2.4 m in our experiment.

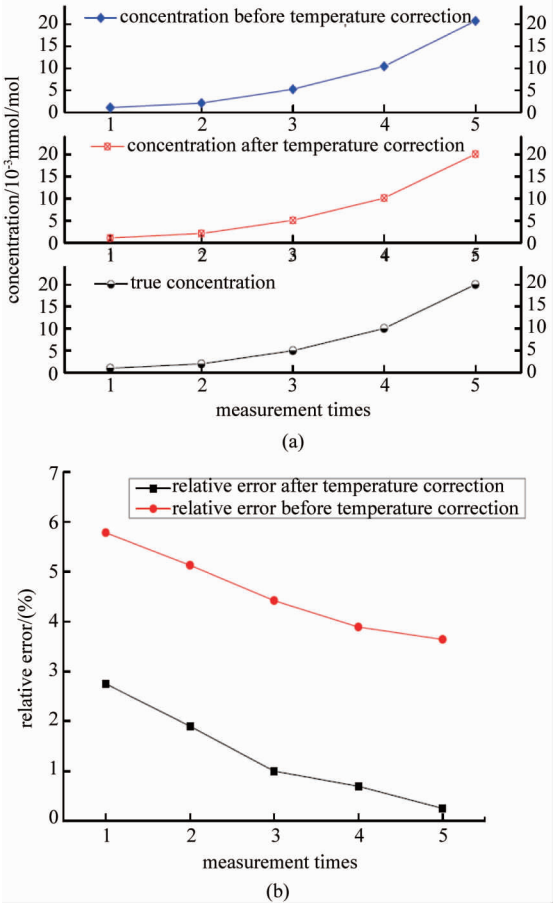

Fig. 4 (a) Concentration results comparison before and after temperature correction, (b) relative error comparison before and after temperature correction
图 4 (a) 温度修正前后的浓度结果比较,(b) 温度修正前后的相对误差比较

3.2 Planting mode

The farmland is at demonstration area in Guoyang, Anhui in China which was chosen as the experimental site on the typical condition of straw returning to the field, and the kind of soil is typical sand ginger black soil. The experiment was carried out in the field from June to December in 2015. This field is a uniform underlying surface as a 700 m × 300 m rectangular area, and the experimental site is essentially flat with no obstructions, as shown in Fig. 5. The prevailing wind here is

Table 2 Results comparison before and after temperature correction
表 2 温度修正前后的结果比较

Ture concentration $\times 10^{-3}$ mmol/mol	Concentration after temperature correction $\times 10^{-3}$ mmol/mol	Concentration before temperature correction $\times 10^{-3}$ mmol/mol	Relative error after temperature correction /%	Relative error before temperature correction /%
1.02	1.048	1.079	2.75	5.78
2.00	2.038	2.103	1.9	5.13
5.01	5.060	5.231	1.0	4.42
10.05	10.120	10.441	0.697	3.89
20.03	20.080	20.759	0.25	3.64

south wind during the experiment.

The wheat straw was returned to the field on June 6th, 2015 and the basic fertilizer was deeply fertilized along with sowing to the soil on June 10th, then the additional fertilizer was broadcast with the rain on July 16th. The corn straw was returned to the field on Oct. 15th, and the basic fertilizer was fertilized along with sowing to the soil on 18th without additional fertilization. The background concentration of ammonia here is about 8.0×10^{-5} mmol/mol.

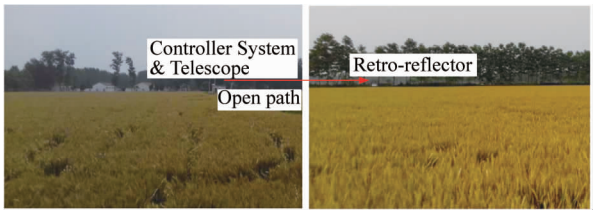

Fig. 5　Experimental site
图 5　实验场地

4　Results and analysis

4.1　Continuous results

The continuous daily average concentration is shown in Fig. 6. It illustrates that the ammonia concentration had an obvious rising trend after fertilization about two weeks; after the additional fertilizer and wheat straw returning in July, the ammonia concentration obviously rose to the peak in August and decreased gradually from September, but it was still higher than that at the beginning of the observation; then it rose again in November after corn straw returning. It illustrates that the concentration rises after straw returning to the field and fertilization. During the experiment, the maximum of the real-time concentration was 2.5×10^{-3} mmol/mol, and the minimum was 3.2×10^{-4} mmol/mol. The performance of OP-TDLAS system was verified as stable and reliable.

The monitoring time was divided into eight periods, and the average concentration of each period was compared and the ammonia volatilization effect with different planting mode was studied, as shown in Fig. 7:

(1) June 1st ~ June 9th-before fertilization and straw returning

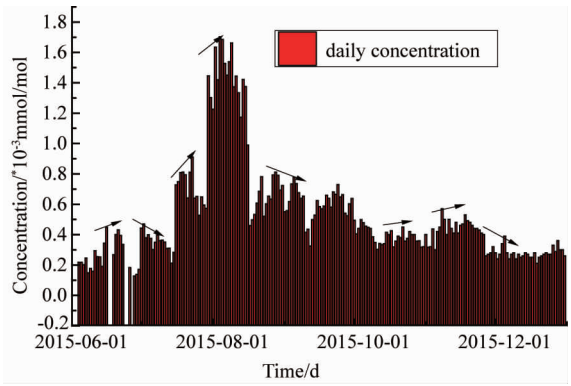

Fig. 6　Continuously monitoring results
图 6　连续监测结果

(2) June 10th ~ June 30th-basic fertilization effect

(3) July 16th ~ July 31st-additional fertilization effect

(4) Aug. 1st ~ Aug. 31st-wheat straw returning effect

(5) Sep. 1st ~ Oct. 15th-weak straw returning effect

(6) Oct. 16th ~ Oct. 31st-basic fertilization effect

(7) Nov. 16st ~ Nov. 26st-corn straw returning effect

(8) Dec. 1st ~ Dec. 31st-weak straw returning effect

Before fertilization and straw returning, the average concentration was low, and it increased after fertilization; one and a half months after wheat straw returning to the field, the daily average concentration rose to the maximum as 1.7×10^{-3} mmol/mol, after four weeks it decreased; one month after corn straw returning, the daily average concentration rose to 4.6×10^{-4} mmol/mol and then decreased again. The maximum daily average concentration with wheat straw returning was about 3.7 times of that with corn straw returning.

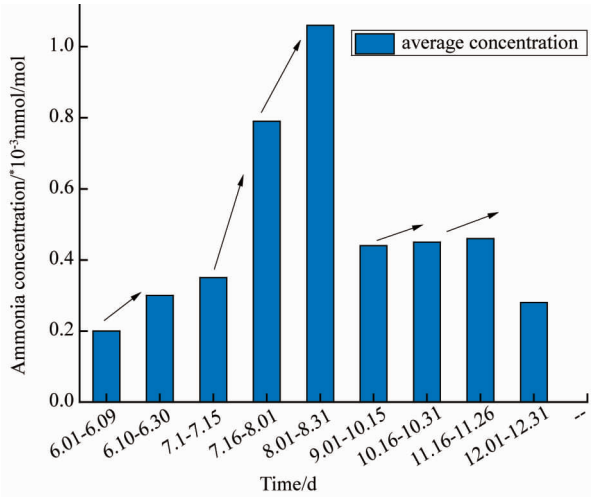

Fig. 7　Monitoring results comparisons between typical periods
图 7　各典型时间区间的测量结果比较

4.2　Seasonal variation

As shown in Fig. 8, there are relatively seasonal variations of NH_3 emissions in the experimental field. The ammonia concentration increased significantly with wheat straw returning in summer, impacted by weather factors and temperature, and the straw stalk rot metamorphic to form the fertilizer. In the same way, the ammonia concentration increased with the corn straw returning, but the ammonia volatilization concentration was lower than that in summer as the temperature reduction in autumn and winter in entirety.

4.3　Diurnal variation

The typical diurnal variations were compared during the observation, as shown in Fig. 8:

(1) June 5th-on behalf of the situation before fertilization and straw returning (background)

(2) June 15th-on behalf of the situation only after fertilization

(3) Aug. 15th-on behalf of the situation after wheat straw returning effect in summer

(4) Nov. 20th-on behalf of the situation after corn straw returning effect in autumn

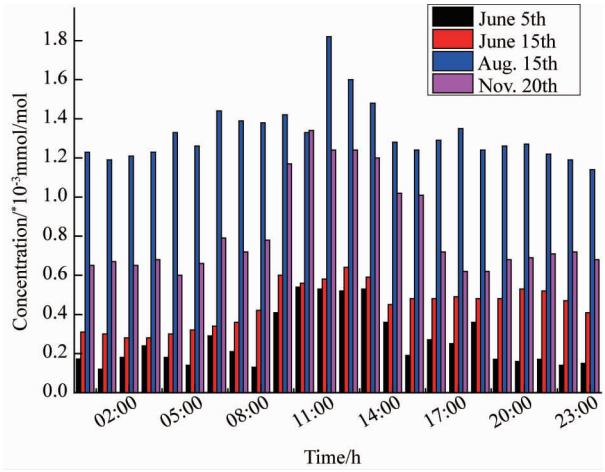

Fig. 8 Variation results comparisons between typical periods
图8 各典型时间区间的日变化结果比较

The ammonia concentration had a same daily variation trend both in summer and autumn, which increased during the daytime and got to the maximum near midday, and then reduced gradually in afternoon and reach to the minimum at night. Ammonia volatilization from soil was closely related to the factors of atmospheric temperature, soil temperature, wind speed and many other meteorological conditions which promote ammonia volatilization. During the observation, the ammonia concentration was relatively low when it is cloudy or windy.

5 Conclusion

In this article, the OP-TDLAS system for NH_3 monitoring has been developed with high sensitivity, rapidly measurement without gas sampling. The quantitative concentration inversion algorithm is mainly studied for characteristic spectrum analysis which was verified to be effective in our experiment. The detection limit of this system is about 4.0×10^{-3} mmol/mol · m.

This OP-TDLAS method was used to obtain the dynamic characteristics of ammonia volatilization concentration from soil of straw returning in Guoyang. As shown by the monitoring results, the ammonia concentration is closely related to straw returning. The daily concentration increases during the daytime and gets to the maximum near midday, and then reduces at night. It increases after straw wheat returning to the field about more than one month impacted by weather factors and temperature at the same time. Moreover, the corn straw returning effect for ammonia volatilization is weaker than the wheat straw returning effect as the low temperature and slow volatilization speed in autumn and winter.

It is verified that this method is able to provide technical support for analyzing the influence of ammonia emissions with straw returning to the field and clarifying the ammonia exchange rule between the soil and the atmosphere.

References

[1] Fowler D, Coyle M, Skiba U, *et al*. The global nitrogen cycle in the twenty-first century[J]. *Philosophical Transactions of the Royal Society of London* 2013, **368**(1621): 91-97.

[2] Gu B J, Ju X T, Chang J, *et al*. Integrated reactive nitrogen budgets and future trends in China[J]. *PNAS*, 2015, **112**(28): 8792-8797.

[3] Vitousek P, Menge D N L, Reed S C, *et al*. Biological nitrogen fixation: Rates, patterns and ecological controls in terrestrial ecosystems [J]. *Philosophical Transactions of the Royal Society of London*, 2013, **368**(1621): 91-97.

[4] Bhattacharyya P, RoyK S, Neogi S, *et al*. Effects of rice straw and nitrogen fertilization on greenhouse gas emissions and carbon storage in tropical flooded soil planted with rice[J]. *Soil & Tillage Research*, 2012, **124**: 119-130.

[5] Petersen S O, Sommer S G. Ammonia and nitrous oxide interactions: Roles of manure organic matter management[J]. *Animal Feed Science and Technology*, 2011, **166-167**: 503-513.

[6] He G X, Li K H, Liu X J, *et al*. Fluxes of methane, carbon dioxide and nitrous oxide in an alpine wetland and an alpine grassland of the Tianshan Mountains, China[J]. *J Arid Land*, 2014, **6**(6): 717-724.

[7] WANG L M, ZHANG Y J, LI H B, *et al*. Study on long distance transmission technique of weak photocurrent signal in laser gas sensor [J]. *Chinese Optics Letters*, 2012, **10**(4): 042802-1-4.

[8] Geng H, Liu J G, He Y B, *et al*. Research on remote sensing of broadband absorbers by using near-infrared diode lasers[J]. *Applied Optics*, 2014, **53**(28): 6399-6408.

[9] Flesch T K, Wilson J D, Harper L A, *et al*. Determining ammonia emissions from a cattle feedlot with an inverse dispersion technique[J]. *Agric For Meteorol*, 2007, **144**: 139-155.

[10] Todd R W, Cole N A, Clark R N, *et al*. Ammonia emissions from a beef cattle feedyard on the southern High Plains[J]. *Atmos Environ*, 2008, **39**: 4863-4874.

[11] Yang Y Y, Liao W H, Wang X J, *et al*. Quantification of ammonia emissions from dairy and beef feedlots in the Jing-Jin-Ji district, China [J]. *Agriculture, Ecosystems and Environment*. 2016, **232**: 29-37.

[12] Yu H Y, Pan J Q, Wang B J, *et al*. Near-infrared distributed-feedback laser sources and system for gas sensing based on TDLAS techniques[C]. *Renewable Energy and the environment*, 2012 OSA, ET4D.7.

[13] Qi R B, He S K, Li X T, *et al*. Simulation of Tdlas direct absorption based on Hitran database [J]. *Spectroscopy and Spectral Analysis*, 2015, **35**(1): 172-177.

[14] Webber M E, Baer D S, Hanson R K. Ammonia monitoring near 1.5 mm with diode-laser absorption sensors[J]. *Applied Optics*, 2001, **40**(12): 2031-2042.

[15] You K, Zhang Y J, Wang L M, *et al*. Improving the stability of Tunable Diode Laser Sensor for natural gas leakage monitoring[J]. *Advanced Materials Research*, 2013, **760-762**: 84.

[16] He Y, Zhang Y J, You K, *et al*. Study on Ammonia Emission rules in a Dairy Feedlot Based on Laser Spectroscopy Detection Method[J]. *Spectroscopy and Spectral Analysis*, 2016, **3**(3): 783-787.